Available online www.ejaet.com

European Journal of Advances in Engineering and Technology, 2021, 8(12):7-12

Research Article ISSN: 2394 - 658X

Microstructure Evolution and Sintering Behaviour of Injection Moulded 316L Stainless Steel Powder

M.A. Omar, N. Johari, M.A. Ahmad and M.J. Sulaiman

SIRIM Bhd, Lot 34, Jln Hi Tech 2/3, Kulim Hi Tech Park, 09000 Kulim, Kedah Malaysia
afian@sirim.my

ABSTRACT

The present study investigates the sintering characteristics of injection moulded gas atomised 316L stainless steel powder using new developed binder system. Model experiments were conducted with new palm-based biopolymer binder system consists of palm stearin and polypropylene. The feedstocks having 65 vol. % of metal powder were injection moulded into a test bar. A rapid two stage debinding process involving solvent extraction and thermal pyrolysis was successful in removing the palm stearin binder in short time. The specimens were then sintered under vacuum atmosphere at the temperature range of 800°C to 1360°C. The sintering studies were conducted to determine the extent of densification and the corresponding microstructural changes. In addition, the properties of the sintered specimens such as physical appearance, microstructure evolution and mechanical properties were presented and discussed. The results showed that as the sintering temperature increased, the sintered properties improve and the powders could be sintered to near-full density.

Key words: sintering, 316l stainless steel powder, density, microstructure

---

INTRODUCTION

Metal injection moulding (MIM) has been widely recognised as an advanced technology for the fabrication of complex-shaped, low cost and high performance components. Fine powders, less than 20 micron in diameter, are mixed with suitable thermoplastic binder and formed into the desired shapes. The binder aids the flowability and formability of fine metal powders during moulding, and they have to be removed in the next stage to enable high density components to be produced. The removal of the binder is done either thermally in the furnace or by solvent extraction. Ideally, the removal of the binder would open up pore channels which allow accelerated removal of the higher boiling point components. The components are sintered following the debinding stage. This stage is crucial to the MIM process as appropriate sintering conditions would ensure pore-free structures that have good mechanical properties [1,2,3,4].

Theoretical studies of sintering treat the powder as a spherical particle and divide sintering into three stages. The early stage of sintering occurs at low temperatures and is characterised by neck growth at the contact points between the particles. The intermediate stage of sintering is characterised by an interconnected pore system having complex geometry. The final stage begins when the pore phase becomes closed and the shrinkage rate of the components slow down. This final stage characterised by pores on four-grain corners that shrink rapidly, and sphereodised powders that separate from grain boundaries and shrink slowly. When all pores on four-grain corners have been eliminated, sintering densification essentially ceases [5,6,7,8].

In previous work, a binder system comprised of parafin wax and thermoplastic binder (polyethylene and polypropylene) as a backbone polymer was successfully mixed and injection molded and has been study by many researchers in the world [3,4,5,6,7,8]. The present study examines the densification process development of MIM 316L gas atomised stainless steel powder using novel palm based biopolymer binder. Palm oil derivative, commonly known as palm stearin, has a major potential application as a component in a binder system in powder injection molding (PIM) process, since it consists of a fatty acid which is commonly used as a surface active agent for many binder systems. Its potential attributes such as low cost, low viscosity and locally availability, have stimulated exploration of its feasibility in the MIM process

MATERIALS AND METHODS

The 316L stainless steel powder used in the experiment was a gas-atomised powder with mean particle size of 12 um and spherical in shape. The powder was mixed with a proprietary biopolymer based binder that consists of palm stearin (PS) and polypropylene (PP) system [9,10,11]. The mixing was carried out in a sigma blade mixer for 1 hour at 160°C before it was removed from the bowl, cooled and then granulated into feedstock. The powder loading was selected at 65 vol. %. The granulated feedstock was fed through the hooper of the vertical injection moulding machine. In the moulding experiments, the temperature and injection pressure was adjusted and the optimum conditions were obtained. The injection specimens were then examined and the dimensions measured in order to determine the linear shrinkage and variation of the moulded specimens.

The green parts were subjected to solvent extraction where around two third of the binder volume fraction was removed. The parts were immersed in heptane for 5 hours at 60°C. Subsequently, the debound specimens were dried at 50°C for about 1 hour to evaporate the heptane from the pores. The parts, which had undergone solvent extraction were subjected to a thermal pyrolysis where all the organic binders were completely removed. The cycle consists of heating at a rate of 5°C/min to 450°C and soaking for 1 hour in vacuum. Sintering of 316L stainless steel powder was carried out in vacuum atmosphere in the range of 800°C to 1360°C with holding time of 2 hours. The physical and mechanical properties were determined using Metal Powder Industries Federation (MPIF) standard method. The microstructure analysis was determined using optical and scanning electron microscopy.

RESULTS AND DISCUSSION

SEM Observation during Presintering

The SEM micrographs of the sample sintered at 800°C to 1300°C are shown in Fig. 1. With the increase in sintering temperature, the boundaries became more thicker indicating that increased the sintering temperature resulted in more active changes at the particles boundaries during sintering.

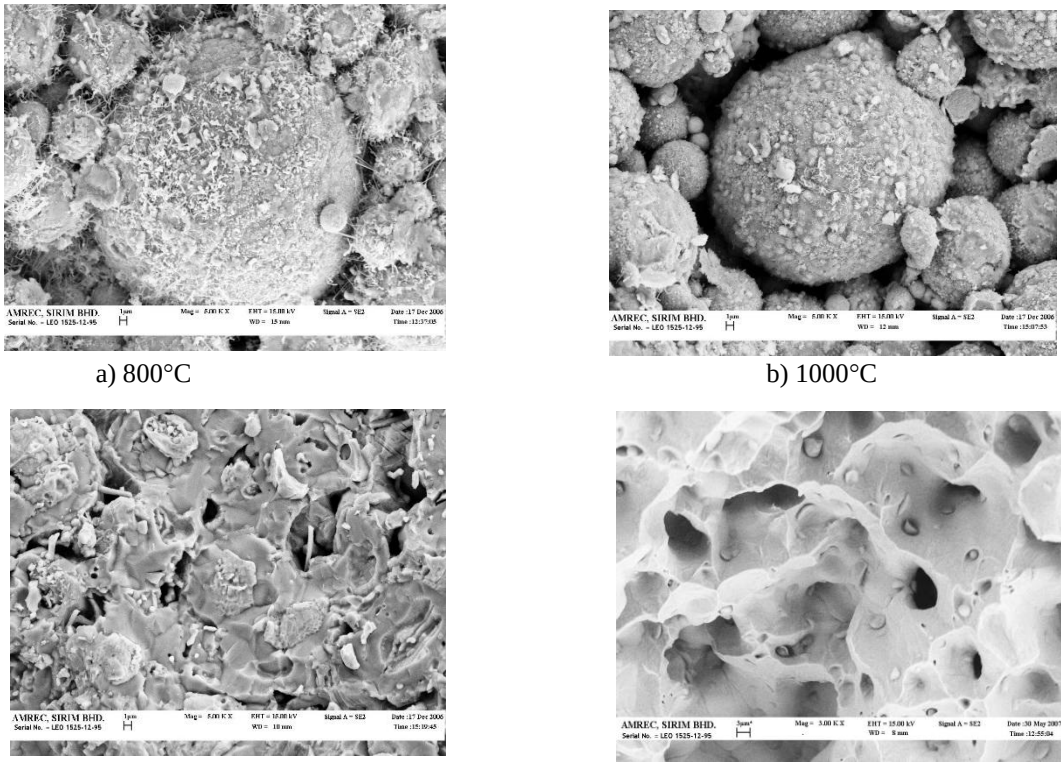

a) 800°C b) 1000°C

c) 1200°C d) 1300°C

Fig. 1 SEM micrographs show the microstructure evolution during sintering process

The SEM micrographs also shows the evidence of poor interparticle bonding at sintering temperature of 800°C and 1000°C. Many particles have just started to form necks. At 1200°C, the sintering process reached the intermediate stage where transport mechanisms such as bulk transport played dominant role. At 1300°C, sintering is likely to be slowed down as during the final stage of sintering, isolated pores start to form and pore rounding.

Effect of Sintering Temperature on Density and Shrinkage

Figure 2 shows the relationship between sintering temperature and the density. As the sintering temperature increased, the sintered density, as expected, increased. Consistent with increasing density, the measured linear shrinkage increased with increasing sintering temperatures.

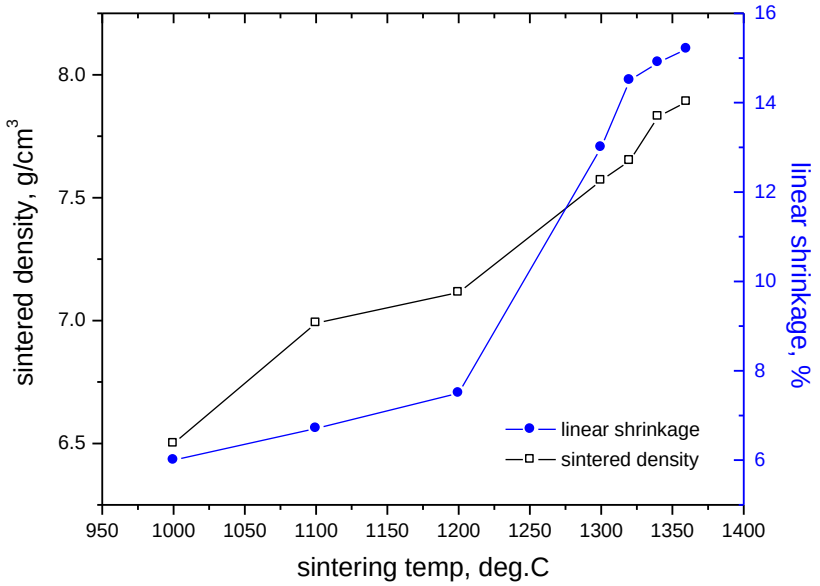

Fig. 2 The effect of sintering temperature on density and linear shrinkage

There is a drastic increase in shrinkage from 1000°C to 1300°C. Increasing the sintering temperature from 1000 to 1300°C enhances the linear shrinkage by 7 %. The sample sintered at 1360°C gave the highest linear shrinkage of about 15%. This indicates that the progress of the first stage sintering (formation of inter-particle necks) at about 1000°C to the final stage at about 1300°C results in significant shrinkage of the samples.

Increasing the sintering temperature from 1300°C to 1360°C enhances the relative density by ~ 4.0%. The sample sintered at 1360°C gave the highest relative density of 99.25%. According to MPIF Standard 35 for Metal Injection Moulded 316L stainless steel, the acceptable percentage level of the theoretical density is 96 – 98%. The present results clearly show that, all samples sintered at 1320°C to 1350°C had densities that exceeded this standard level and that the 1360°C samples had values that exceeded the maximum of the standard range. At that temperature sintering is likely to be slowed down as during this final stage of sintering, isolated pores started to form. Hence densification of the parts will reach certain level with respect to the increase in sintering temperature after which the shrinkage will level off and grain growth takes over.

The increased in density with increased sintering temperature is accompanied by an increased in in grain size and by gradual closing of pores as expected. Figure 3 show the microstructures of etched samples sintered at 1300°C and 1360°C. These show how the substantial grain growth occurred at the highest sintering temperature.

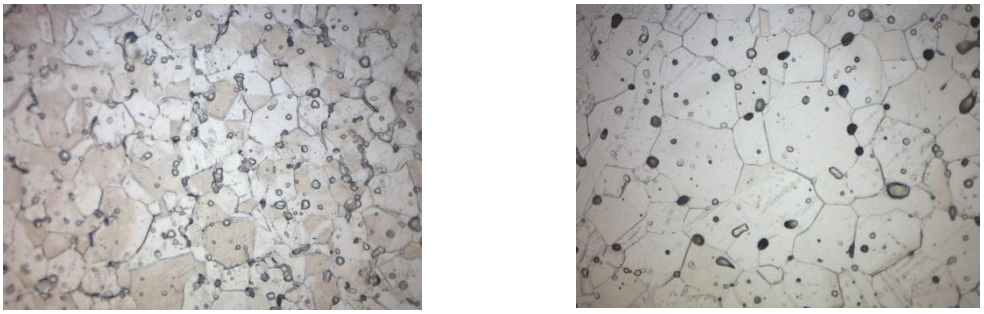

a) 1300°C b) 1360°C

Fig. 3 Optical micrographs show the microstructure at different sintering temperature

Figure 4 illustrates the effect of sintering temperature on the hardness and tensile strength. It is clearly shown that increasing the sintering temperature increased the hardness and strength of the sintered specimen presumably due to better densification. The hardness increased from 120 Hv for the moulding sintered at 1000°C to 380 Hv for the moulding sintered at 1350°C. The increased in hardness is accompanied by an increased in tensile strength. A substantial increased in strength (about 100%) is observed when the sintering temperature in increased from 1000°C to 1300°C

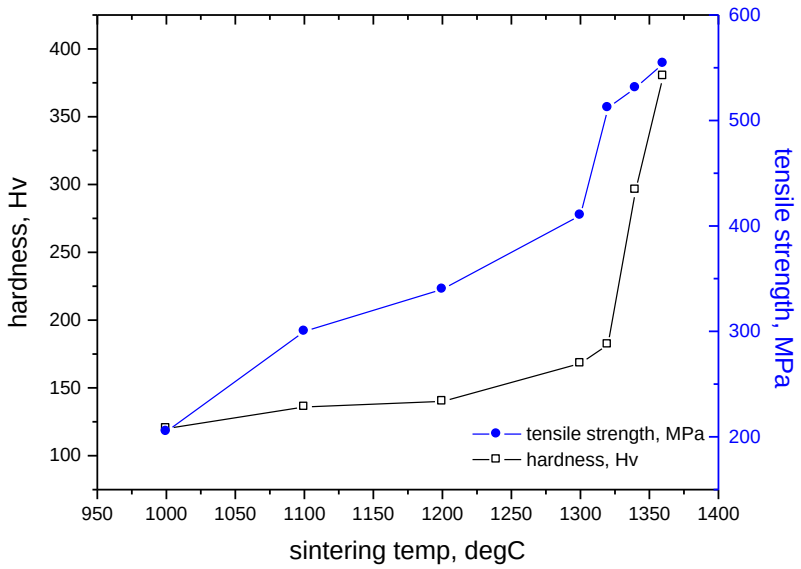

Fig. 4 The effect of sintering temperature on the hardness and tensile strength

The acceptable sintered tensile strength for 316L stainless steel produced by an MIM process, according to MPIF Standard 35, is 480 MPa or greater. It clearly shows that sintering at the temperature of 1320°C to 1360°C resulted in a tensile strength of greater 480 MPa. Figure 4 also shows the hardness of the sintered parts as a function of sintering temperature. It is evident that a sintering temperature of 1360°C resulted in the highest hardness for all the sintering temperature used. MPIF Standard 35 specifies that hardness for 316L stainless steel should be ~ of 200 HV. From the hardness result obtained, the appropriate sintering temperature for 316L stainless steel powder using the palm based binder content of palm stearin appears to be 1320°C to 1360°C respectively. An appropriate sintering temperature for optimal mechanical properties appears to be 1360°C.

During sintering, the initially loose powder compact undergoes a transformation to become a dense, polycrystalline structure with physical and mechanical properties similar to engineering materials. The final stage of sintering has a few pores sitting on grain boundaries. Figure 5 depicts the SEM fractographs of vacuum sintered SS 316L specimens at different temperatures ranging from 1300^{o}C to 1360^{o}C. At 1300^{o}C, it clearly shows that the powder boundaries were replaced by grain boundaries as shown in Figure 5 (a). As the temperature was increased, the microstructure began to coarsen that considerable reduction of surface area, increase in grain size and compact strengthening with attendant changes in the pore size and shape.

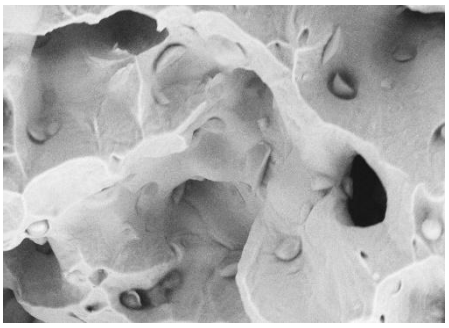

(a) 1300 ^{o}C

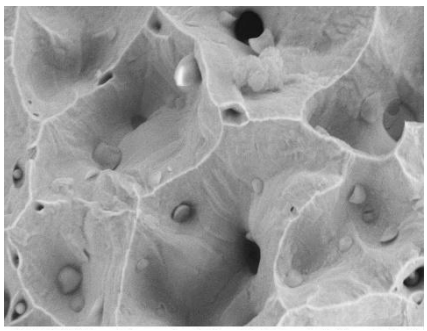

(b) 1320 ^{o}C

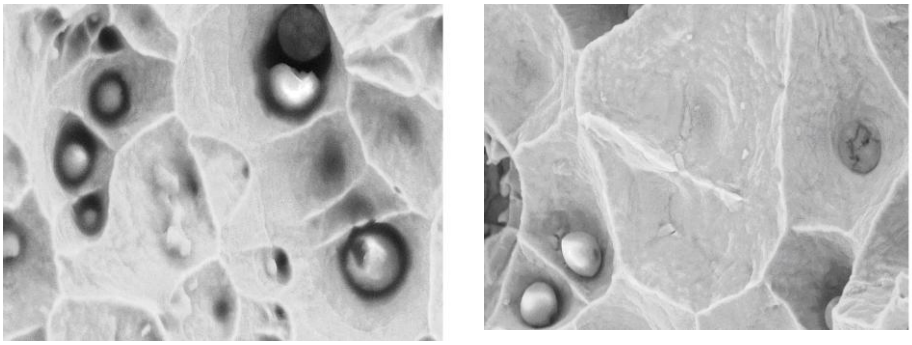

(c) 1340 ^{o}C (d) 1360 ^{o}C

Fig. 5 SEM fractographsshowing the fracture surface of 316L SS specimen sintered at various temperatures

Sample sintered at 1320^{o}C shows spherodising of pores and shrinking, which are not connected to the compact surface (Figure 5(b)). These pores are termed closed pores. The pore located on grain boundaries as shown in Figure 5(a) disappeared as temperature increased, but pores disconnected from grain boundaries remain stable as shown in Figure 5(c) and (d). The typical ductile fracture mechanisms is evidence by dimples in the final stage of sintering as can be seen in Figures 5(c) and (d). A few isolated pores (closed pores) can also be observed in the Figures 5(c) and (d) suggesting that closed pores play little part in the fracture. These closed pores are sealed and inaccessible via the sintering atmosphere.

There are many fine particles that appeared in the centre of a grain boundary. These particles have a dimension of approximately 3 µm. As shown in Figure 6, the energy dispersive spectroscopy (EDS) result shows that this is the particles which is not diffused and appeared exclusively. Table 1 shows the elements found in the particles.

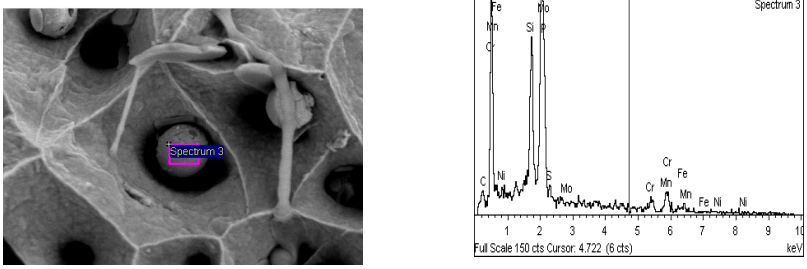

Fig. 6 EDS of sintered specimen

Table -1 Element present in the fine particles

Element	**C**	**Si**	**P**	**S**	**Cr**
Weight %	4.3	13.7	5.7	3.6	61.4
Element	**Mn**	**Fe**	**Ni**	**Mo**	**Total**
Weight %	0.0	11.3	0.0	0.0	100.0

The specimens sintered at lower sintering temperatures still show particulate features and open pores. At lower densities or temperatures, main fracture mode is the separation of particles at necking areas where bonding between particles took place during sintering. With increasing density, increased ribbed features are seen on the fractured surfaces indicating some grains fail in ductile mode. At the 1300 °C, both closed pores and open pores connected together attributed to lower strength of samples. On the other hand, typical ductile fracture mechanism evidenced by dimple is noted in Fig. 5.

CONCLUSION

The sintering process of injection moulded 316L stainless steel specimen is clearly influenced by sintering temperature. With a high sintering temperature, the density shrinkage, tensile strength and the hardness of the sintered specimens increase due to the pore shrinkage. The closure of the pores enhanced the mechanical properties of the sintered samples. From this study, it can be concluded that the best sintering temperature for the 316L stainless steel powder using palm based binder is 1360 °C which result in good properties for the sintered parts, and comply with the requirement for MPIF Standard 35 for Metal Injection Moulded Parts.

REFERENCES

[1]. R.M. German and A. Bose, Injection Moulding of Metals and Ceramics, MPIF, Princeton, NJ. (1997)

[2]. R.M. German and R. Cornwall. “The Powder Injection moulding Industry: An Industry and Market Report”, Innovative Materials Solution Inc, Pennsylvania, (1997)

[3]. R.M. German, K.F.Hens, and S.T. Lin,. Ceramic Bulletin. Vol.70 (1991), 8, 1294-1301
[4]. M.A.Omar., Davies, H.A., Messer, P.F., Ellis, B. (2001). The influence of PMMA content on the properties of 316L Stainless Steel MIM Compact, *Journal of Materials Processing Technology* 113: pp 477-481.
[5]. M. A. Omar, I. Subuki, N. S. Abdullah, N. Mohd Zainon and N. Roslani, "Processing of Water-atomised 316L Stainless Steel Powder Using Metal-injection Processes", Journal of Engineering Science, 2012, Vol. 8, 1–13
[6]. M. A. Omar*, S. Ibrahim, N. Johari, N. Abdulah and N. M Zainon, Processing and In-Vitro Study of Injection Moulded Cocrmo Alloy Hip Stem for Orthopedic Applications, Saudi J EngTechnol, June 2019; 4(6): 243-247
[7]. Standard Test Methods for Metal Powder and Powder Metallurgy Products, MPIF, Edition, Princeton, NJ (1992)
[8]. ISO/EN 10993-5: Biological evaluation of medical devices – Part 5: Test for Cyctotoxicity: in-vitro Method
[9]. Omar, M.A., and Subuki, I., (2007) Rapid Debinding of 316L Stainless Steel Injection Moulded Using Palm Based Biopolymer Binder, Proceedings of 3rd Cooloquium on Postgraduate Research on Materials, Minerals and Polymers 2007, Vistana Hotel, Penang
[10]. Omar, M.A., Subuki, I. and Ismail, M.H., (2006). Observation of Microstructural Changes during Solvent Extraction and Polymer Burnout Process of MIM Compact", Proceedings of 5th International Materials Technology Conference and Exhibition 2006 (IMTCE 2006), July, 2006, Kuala Lumpur
[11]. Omar, M.A., (2006). Metal injection Moulding- An Advanced Processing Technology", *Journals of Industrial Technology*, 15 (1), 11-22